Journal Pre-proofs

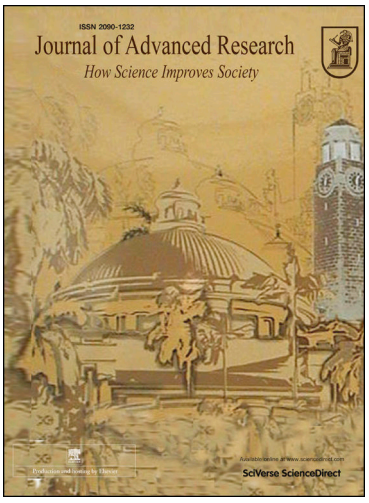

A hybridized mechano-electroporation technique for efficient immune cell engineering

Dorsa Morshedi Rad, William P. Hansen, Sareh Zhand, Charles Cranfield, Majid Ebrahimi Warkiani

PII: S2090-1232(23)00346-6
DOI: https://doi.org/10.1016/j.jare.2023.11.009
Reference: JARE 1490

To appear in: *Journal of Advanced Research*

Received Date: 16 April 2023
Revised Date: 16 October 2023
Accepted Date: 10 November 2023

Please cite this article as: Morshedi Rad, D., Hansen, W.P., Zhand, S., Cranfield, C., Ebrahimi Warkiani, M., A hybridized mechano-electroporation technique for efficient immune cell engineering, *Journal of Advanced Research* (2023), doi: https://doi.org/10.1016/j.jare.2023.11.009

A hybridized mechano-electroporation technique for efficient immune cell engineering

Dorsa Morshedi Rad[a], William P. Hansen[b], Sareh Zhand[a], Charles Cranfield[b], Majid Ebrahimi Warkiani*[a,c]

[a]School of Biomedical Engineering, University of Technology Sydney, Sydney, NSW 2007,

[b] School of Life Sciences, University of Technology Sydney, Sydney, NSW 2007,

[c]Institute for Biomedical Materials and Devices (IBMD), Faculty of Science, University of Technology Sydney, Sydney, NSW, 2007, Australia

Credit Authorship Contribution statement

Dorsa Morshedi Rad: Conceptualization, investigation, and writing the original draft, **William P. Hansen:** Investigation and writing the original draft, **Sareh Zhand:** investigation, **Charles Cranfield:** Supervision, review and editing the draft, **Majid Ebrahimi Warkiani:** Conceptualization, supervision, funding acquisition, and review and editing the draft.

*Contact

Majid Ebrahimi Warkiani (majid.warkiani@uts.edu.au)

School of Biomedical Engineering, University Technology Sydney, Sydney, New South Wales 2007, Australia

A hybridized mechano-electroporation technique for efficient immune cell engineering

Abstract

Immune cell engineering, which involves genetic modification of T cells, natural killer cells, and macrophages, is shifting the paradigm in immunotherapy for treating hematologic malignancies. These modified cells can be viewed as living drugs and offer advantages, including dynamic functionality, active local trafficking, and boosting the immune system while recognizing and eliminating malignant cells. Among the current technologies employed for the modification of immune cell functions, electroporation stands as a predominant approach, but it suffers from heterogeneity arising from the treatment of a bulk population of immune cells during the manufacturing procedures. To address this challenge of the field, here we present a hybrid approach to induce consecutive gentle mechanical and electric shocks. This approach enhances the treatment homogeneity and improves outcomes in difficult-to-load immune cells. The hybrid approach aims to enhance the treatment homogeneity by passing individual immune cells through a microengineered filter membrane with micropores smaller than the cell diameter. This facilitates the creation of transient pores in the cell membrane, followed by efficient delivery of biomolecules through the complementary use of a gentle electric shock. Using this hybrid mechano-electroporation (HMEP) system, we could successfully deliver fluorescein isothiocyanate (FITC) dextran molecules from the smallest (4 kDa) to the largest (2000 kDa) size and GFP expressing plasmid DNA into different immune cell types. We also provide insight into the delivery performance of the HMEP system in comparison with the benchtop electroporation since both methods hinge on membrane disruption as their permeabilization mechanism. Immune cells treated with the HMEP protocol demonstrated higher delivery efficiencies while maintaining cell viability compared to those experiencing conventional electroporation. Therefore, membrane-based mechanoporation can be a cost-effective and efficient approach to pre-treat the hard-to-deliver immune cells before electroporation, elevating the treatment homogeneity and delivery of exogenous cargoes to a higher level.

Keywords: *Membrane disruption; Hybrid mechano-electroporation protocol; Immune cell engineering; Cancer immunotherapy*

1. Introduction

Cancer is a life-threatening malignancy accounting for one in every six deaths worldwide [1]. For decades, cancer treatment options were limited to surgery, chemotherapy, radiotherapy, or combination therapy, which takes advantage of two or more therapeutics to target cancer cells [2, 3]. However, conventional treatments are associated with problems such as high cost and cytotoxic effects on both cancer and normal cells. Therefore, recent efforts have gone into developing personalized therapies that can only eliminate cancer cells without affecting normal cells [4]. Immunotherapy marks the beginning of a new era in cancer treatment, as it harnesses the patient's coordinated and adaptive immune system to eliminate cancer [5].

Since its conception, immunotherapy has been successful in treating many diseases, from cancer to cardiovascular, neurological, and hematological disorders [6, 7]. To date, different types of

immunotherapies have been developed, including cytokine-based immunomodulation (e.g., IL-2 and IF-α), therapeutic vaccines, oncolytic viruses, immune checkpoint blockade, and immune cell engineering [8]. Among these, immune cell engineering (also known as cell-based immunotherapy) has been recognized as the most promising therapeutic approach owing to its effectiveness with minimal off-targeting and other side effects [9].

To date, different modalities have been used in cell-based immunotherapy, such as viral vectors (e.g., lentiviruses and adeno and adeno-associated viruses), electroporation, microfluidics, nanoparticles, and nanostructures [10-13]. While viruses can result in high delivery efficiencies, issues such as immunogenicity, limited packaging capacity, required specificity for genetic cargo, and high cost have limited their use in clinical settings. Additionally, cells can destroy or reject large amounts of delivered cargo, lowering the final delivery efficacy [14]. Electroporation has been a well-known strategy for delivering a wide range of payloads into various cell lines. However, previous studies have reported a subsequent low proliferation rate resulting from significant changes in the expression level of stress-related genes upon electroporation [12, 15].

Recent delivery technologies have assisted microfluidics in manipulating the cells within microchannels and creating transient pores in the cell membrane [16]. Microfluidic-based delivery technologies, including cell squeezing, hydroporation, and mechanoporation, have been used to load biomaterials into the target cells with minimal effects on cell viability and proliferation post-treatment [17-20]. However, low throughput, treatment inconsistency and heterogeneity, as well as device-blocking issues, remain the main challenges of these technologies [21]. Among these, mechanoporation using microfilters, also called microfiltroporation, has been recently optimized for delivery purposes with the potential of addressing the heterogeneity of treatment and blocking issues of conventional mechanoporation strategy using polycarbonate track-etched filters [22, 23]. Previous studies have employed filter membranes to transiently open pores across the plasma membrane and facilitate cargo internalization into the cells of interest. This approach has successfully loaded FITC dextran molecules of different sizes ranging from 4 to 2000 kDa into both adherent and suspended cell lines [20, 23]. Furthermore, microfiltroporation has demonstrated potential in gene-editing of hematopoietic stem cells through nuclear internalization of the CRISPR/Cas9 ribonucleoprotein complex that targets β2-microglobulin [22]. Since microfiltroporation offers a cost-effective and user-friendly delivery solution, it is worth exploring the synergistic effects of microfiltroporation and other membrane permeabilization methods. This may result in establishing a highly efficient delivery strategy that mitigates the problem of treatment heterogeneity.

Here, for the first time, we propose using a cost-effective, hybrid delivery approach that utilizes successive mechanical and electric shocks to the immune cells to enhance delivery outcomes beyond those achieved by each membrane disruption technique individually. In this hybrid mechano-electroporation or HMEP approach, we utilized microfiltroporation followed by electroporation and demonstrated how these two methods could be synergistically employed to enhance immune cell permeabilization and engineering to a greater extent. The HMEP system introduces a mixture of immune cells and delivery molecules into a silicon nitride (SiN) microsieve, which mechanically disrupts the cell membrane. This is followed by an electric shock to further enhance membrane disruption, resulting in transient membrane permeabilization and efficient internalization of a diverse range of exogenous cargoes (4-2000 kDa FITC dextran and GFP expressing plasmid DNA) into immune cell lines that are usually difficult to transfect. The

HMEP method offers high delivery efficiency (up to 98%) with minimal cell perturbation (up to 94%). Its potential for implementation in immune cell engineering at clinics is promising, given its high throughput (1-5×10^6 cells min^{-1}), simplicity, and immediate delivery.

2. Materials and methods

2.1 Microfabrication process

The SiN (Si_3N_4) microsieves were fabricated using double-sided silicon wafers in collaboration with Aquamarijn (ZT, NL). First, the silicon substrate was deposited on both sides of the silicon wafers, followed by potassium hydroxide dipping to wash away the residual silicon and achieve the desired thickness (~1μm). This was followed by patterning arrays of circular micropores on silicon wafers through the standard photolithography and reactive ion etching as described previously [23].

2.2 Cell lines and culture preparation

Human immune cell lines included Jurkat (representative of T lymphocytes), THP1, and Molm-13 (representative of monocytes), as well as Raji cells (representative of B cells), were purchased from ATCC (VA, USA). The immune cell lines were cultured using standard protocols in RPMI-1640 media (Life Technologies, MA, USA) with 10% FBS (Life Technologies, MA, USA) and 1% GlutaMAX (Life Technologies) and grown on a steady surface at 37°C in a humidified atmosphere with 5% CO2 [24]. The cell proliferation and viability were monitored via BIORAD TC20 Automated Cell Counter (Bio-Rad, CA, USA). Before performing any experiment, cells were washed three times with DPBS (Life Technologies, MA, USA) and resuspended in the desired buffer containing the delivery material.

2.3 Delivery materials

FITC dextran molecules ranging from 4-2000 kDa were used as representatives of delivery materials (Sigma Aldrich, MO, USA). The EGFP-expressing plasmid DNA (pEGFP-C1, Catalog # 6084-1, Addgene) was kindly gifted by Prof. Deborah Marsh and was used to prove the ability of the hybrid approach to deliver functional biomolecules. The immune cell suspension was mixed with 5 μM of the FITC dextran molecules and 1 μg of the EGFP-expressing plasmid DNA to be subjected to the HMEP system and evaluate the delivery performance of the HMEP system. Next, the HMEP-treated cells were cultivated following the standard protocols [24].

2.4 HMEP delivery system and optimization

To find the optimal delivery conditions using HMEP, we first optimized the treatment sequence by evaluating whether the immune cells should first experience a mechanical or electric shock. For this purpose, we tested two different sequences: electroporation followed by mechanoporation (electroporation → mechanoporation) and mechanoporation followed by electroporation (mechanoporation → electroporation). The electroporation and mechanoporation parameters were chosen according to the previously published protocols [23]. We first optimized each treatment separately to determine the optimal delivery conditions, followed by optimizing the mechano-electric coupling conditions. To this aim, cell suspensions containing immune cells and delivery

cargoes were electroporated using the Neon™ Transfection System (Thermo Fisher Scientific Inc, MA, USA) under different voltages (1.05-1.45 kV), durations (10-20 ms), and the number of electric pulses (1-3×). To optimize mechanoporation or microfiltroporation, the immune cell suspension containing delivery materials was directed through SiN microsieves with micropores smaller than the cell size. This involved passing the cell suspension through the micropores at varying speeds, using a range of flow rates between 0.5 to 2 ml min^{-1} to induce transient membrane disruptions. To ensure the validity, repeatability, and consistency of the results, all experiments were performed in triplicate.

2.5 Immune cell permeabilization and delivery procedure

Immune cell membrane permeabilization and delivery were carried out following established methods from prior publications [23]. In brief, immune cells were centrifuged at 500×g for 3 minutes, then resuspended in the DPBS (delivery buffer) to make a final concentration of $1\text{-}5\times10^6$ cells ml^{-1}. Next, the delivery solution, containing the desired immune cells and delivery molecules, was loaded in a 3 mL syringe (Becton-Dickinson, MA, USA) and pumped through the SiN membranes (fabricated in collaboration with Aquamarijn, ZT, NL) with 5 µm pores to induce mechanical shock followed by electroporation under the optimized testing conditions. Finally, the treated immune cells were collected in 1.5 mL Eppendorf tubes and incubated at 37°C for a few minutes to allow plasma membrane repair/recovery.

2.6 Flow cytometry analysis

Upon recovery, treated immune cells were centrifuged into a pellet at 500×g for 3 minutes and washed with DPBS twice to remove excessive delivery material, media, or cell debris. The immune cell pellet was resuspended in FACS buffer (DPBS+5% FBS+1% F-68). A 1:1000 dilution of viability dye -SYTOX™ Blue dead cell stain (Thermofisher Inc, MA, USA) was then added to the FACS buffer under light-sensitive conditions [25]. Then, the flow cytometry and data analysis were carried out using the BD FACS LSR Fortessa cell analyzer and BD FACSDiva™ software (Becton-Dickinson, MA, USA), respectively. Using SYTOX blue (excitation/emission: 444/480nm) and FITC dextran molecules (excitation/emission: 495/521 nm), the emissions of specified wavelengths were measured, indicating cell viability and delivery efficiency, respectively.

2.7 Fluorescent microscopy

The THP1 cells treated with HMEP and loaded with a GFP-expressing plasmid were seeded into a 6-well plate containing complete media. After 48 hours, the cells were examined using fluorescent microscopy with an EVOS M5000 imaging system (Thermofisher Inc, MA, USA).

2.8 Cell membrane damage analysis via Lactate dehydrogenase (LDH) assay

To evaluate the cell membrane injury induced by the HMEP delivery system, 48h post-treatment, the supernatant of control, electroporated, and HMEP-treated cells were collected. These samples were then employed for lactate dehydrogenase assay (LDH) using the CyQUANT™ LDH Assay (Thermo Fisher Scientific Inc, MA, USA) according to guidelines for evaluating cell viability and membrane integrity [26]. LDH activity was measured based on the light absorption of the culture

supernatant at two wavelengths of 490 and 680 nm with Varioskan Lux Reader (Thermo Fisher Scientific Inc, MA, USA) according to the manufacturer's protocol.

2.9 Cell proliferation analysis via MTS assay

48h hours post-treatment, control, electroporated, and HMEP-treated samples were seeded at the density of 10,000 cells ml^{-1} in wells of a 96-well plate (Corning, NY, US) to evaluate the effect of the HMEP delivery system on cell proliferation. An MTS ((3-(4,5-dimethylthiazol-2-yl)-5-(3-carboxymethoxyphenyl)-2-(4-sulfophenyl)-2H-tetrazolium)) assay was performed on these cells using the CellTiter 96® AQueous One Solution kit (Promega, WI, US) according to the manufacturer's protocol and guidelines for evaluating cell viability and membrane integrity [26]. The cell proliferation was measured based on the detected absorbance at 590 nm using the Varioskan Lux Reader (Thermo Fisher Scientific Inc, MA, USA).

2.10 Cell viability and apoptosis assay

The cell viability analysis was performed at the time of the experiment and 48h post-treatment using the SYTOX™ Blue dead cell stain (Thermofisher Ins, MA, USA) and flow cytometry to exclude live and dead populations of the cells. To determine the number of apoptotic cells 48h post-treatment, an apoptosis assay using FITC Annexin V (Biolegend, CA, USA) was performed according to the manufacturer's protocol and guidelines for evaluating cell viability and membrane integrity [26].

2.11 Cytokine array

The cytokine array analysis was performed 72h post-treatment using the human cytokine antibody array (ab133996, Abcam, USA) on electroporated and HMEP-treated cells. This analysis aimed to evaluate the functionality of the cells and their response to the treatment. For this purpose, the non-treated control and HMEP-treated samples were incubated for 48 h at 37ºC temperature in a humidified atmosphere with 5% CO2. Following incubation, the conditioned medium was collected and subsequently used for cytokine array analysis according to the manufacturer's protocol, which profiles 23 human antibody targets.

2.12 Statistical analysis

The statistical analysis involved a one-way analysis of variance (ANOVA) for multiple comparisons, followed by post-hoc Holm-Sidak tests. These tests were used to compare the independent variables or factors, namely electroporation and HMEP, in relation to the dependent variables of delivery efficiency and cell viability. GraphPad Prism software 6. *P*-values<0.05 were considered statistically significant and displayed as **P*-value. **, ***, and **** indicated *P*-values<0.01, 0.001, and 0.0001, respectively.

3. Results and Discussion

3.1 Treatment sequence in the HMEP system

While microfiltroporation has been successfully utilized for the permeabilization of several commonly used mammalian cell lines, its optimization for immune cell permeabilization remains an unexplored area. Furthermore, the potential synergies between microfiltroporation and other membrane permeabilization techniques, such as electroporation, have not received substantial attention. Immune cells have demonstrated a high degree of tolerance to cargo internalization, even in the context of using membrane permeabilization technologies that have been successful in cargo delivery to other cell types [27]. This tolerance might be attributed to distinctive features of immune cells, including their phospholipid bilayer composition and membrane properties, efflux mechanisms expelling foreign biomolecules, and enhanced cellular defense mechanisms [28]. Further investigations are required to comprehensively understand these distinctions and to enhance cargo delivery to immune cells effectively.

To address the current gap in effective cargo delivery to immune cells, we aimed to investigate whether the addition of an electric shock into the microfiltroporation process could improve the delivery outcomes. To achieve this, we proposed an HMEP delivery platform consisting of two functional units: mechanoporation and electroporation. While facilitating more homogeneous cargo delivery, this platform introduces milder electric shocks to the cells, eliminating the potential side effects. To optimize the treatment sequence for cargo delivery to immune cells, we tested two different conditions. First, we performed electroporation followed by mechanoporation (electroporation → mechanoporation, Figure 1A). We then tested the reverse order by passing the immune cells through the SiN microsieves before applying a gentle electric shock (mechanoporation → electroporation, Figure 1B). During the mechanoporation, immune cells and delivery material were forced through the micropores of SiN membranes. These micropores are designed to be smaller than the cell diameter, inducing mechanical cell perturbation and facilitating the transient pore formations. Based on our previous observations, the flow rate of 2 ml min^{-1} was adopted as the optimal speed to pass the mammalian cells through the SiN microsieves, resulting in a trade-off between cell viability and delivery efficiency [23]. Therefore, in each combination of experiments, mechanoporation was performed at the optimal operational flow rate, and electroporation parameters were chosen according to the manufacturer's protocol (1.35 kV, 10 ms, and 3 pulses).

As a result, our findings demonstrated that priming Jurkat cells with mechanoporation prior to the electroporation resulted in higher cell viability (~70%) and improved loading efficiency of 4 kDa FITC dextran (~85%), as depicted in Figure 2. These results effectively replicate the delivery of smaller cargo molecules such as siRNA and antibodies. Notably, in a previous study conducted by Raes *et al.*, a lower delivery efficiency (~60%) was achieved when loading 4-10 kDa FITC dextran into Jurkat cells using the vapor nanobubble photoporation approach. Photoporation, also known as optoporation, is a membrane disruption technique that employs laser light to transiently create pores in the plasma membrane [29]. In a separate investigation conducted by O'Dea et al., they employed a reversible permeabilization technique, utilizing low levels of permeabilizing agents such as ethanol, to induce membrane disruption and deliver 4-10 kDa dextran-Alexa488 into Jurkat cells. However, this method yielded a delivery efficiency of less than 60% for loading this cargo into the Jurkat cells [30].

While photoporation, reversible permeabilization, and the HMEP approach all employ membrane disruption mechanisms, there exists a difference in the delivery outcomes. This suggests that a sequential combination of mechanical and electrical disruption of the immune cell membrane can enhance delivery outcomes while minimizing cell damage. Future studies should aim to assess the impact of pre-treating Jurkat cells with microfiltroporation prior to implementing photoporation or reversible permeabilization and evaluate its effect on delivery outcomes. This further investigation holds the potential to illuminate the synergistic interactions between these membrane disruption methods. Moreover, our findings revealed that the effectiveness of the HMEP platform did not rely on the specific properties of the delivered molecules. This was evident through the demonstration of passive diffusion mechanisms that governed the internalization of exogenous cargo. Importantly, passive diffusion operates without the requirement for carriers or the expenditure of active energy [31].

3.2 Optimization of the HMEP delivery conditions

Several parameters affect the delivery performance of the HMEP platform, including the speed of passing the immune cells through the micropores and electric field intensities. To find the optimal delivery conditions, we performed several experiments to characterize the cytoplasmic delivery of 4 kDa FITC dextran into Jurkat cells using electroporation and mechanoporation separately. To optimize the electroporation protocol, experiments were conducted using two different cell lines, THP1 (Table 1) and Jurkat (Table 2). A wide range of voltages with different wavelengths and frequencies were tested to determine the optimal conditions that would allow efficient loading of the 4 kDa while maintaining cell viability for both cell lines. Based on the findings presented in Figure 3A, it was observed that electroporation of Jurkat cells at 1.35 kV for 10 ms and 3× resulted in successful loading of over 75% of the Jurkat cells with the 4 kDa FITC dextran while more than 90% were viable. This outcome aligns closely with the manufacturer's recommendations, as suggested in their guidelines [32]. The results of the mechanoporation optimization experiments using the same cell line and delivery cargo shown in Figure 3B demonstrated that at the flow rate of 2 ml min^{-1}, more than 87% of the Jurkat cells were successfully loaded with the desired cargo, which is consistent with the previously published literature [23].

To optimize the delivery conditions of the HMEP protocol, Jurkat cells were subjected to a range of flow rates while they were passing through the SiN microsieves, followed by electroporation under the optimized conditions (Figure 3C). The results shown in Figure 3D demonstrate that mechanoporation at flow rates of 0.5 and 1 ml min^{-1} followed by electroporation could successfully deliver 4 kDa FITC dextran with high efficiency, achieving up to 96% and 75.5% cytoplasmic delivery, respectively. Based on these findings, both flow rates were selected as the optimal parameters for the mechanoporation unit in the HMEP protocol for subsequent experiments. Importantly, the HMEP protocol utilizes lower flow rates in the mechanoporation unit to prime the cells before electroporation, reducing potential cellular stress while creating transient membrane pores and facilitating consistent cytoplasmic delivery. In a study conducted by Ding et al., they introduced an innovative delivery method that combined cell squeezing and microelectroporation. This approach involved the integration of a device equipped with constrictions smaller than the cell diameter for cell squeezing and microelectrodes for microelectroporation. In their study, they observed that subjecting cells to higher squeezing speeds led to the generation of larger membrane ruptures, which, in turn, impacted cell viability [33]. This observation aligns with our findings, as we also achieved higher cell viability when employing

lower flow rates. Future investigations can further explore membrane disruption and repair mechanisms involved in HMEP-mediated membrane permeabilization.

3.3 HMEP-mediated cargo delivery into human immune cell models

To validate the delivery performance of the HMEP protocol under the optimized operational conditions, we delivered 0.4 mg ml^{-1} of FITC-conjugated dextrans of different sizes into various immune cell lines. Subsequently, we employed flow cytometry analysis to quantitively assess the delivery outcomes immediately after the treatment. In addition, we conducted a comparative analysis to assess the cytoplasmic delivery efficiency between the HMEP protocol and conventional electroporation. This comparison was based on their shared mechanism of action, which revolves around membrane disruption. For our analysis, we selected Jurkat cells (human T lymphocytes) as it is a well-documented hard-to-transfect human lymphocyte [34, 35]. It is important to highlight that we chose immune cell lines known for their difficulty in permeabilization for this study. Consequently, the successful delivery of cargo molecules using the proposed hybrid strategy could provide a rapid and efficient solution for immunotherapy in clinical settings.

Our observations showed that Jurkat cells were efficiently loaded with the 4 kDa FITC dextran (approximately the size of a small molecule drug or siRNA) when compared to the endocytosis control. Although the HMEP protocol demonstrated slightly higher delivery efficiencies (~8.5%) for the cytoplasmic loading of 4 kDa FITC dextran into Jurkat cells compared to electroporation, the cell viability was similar for both platforms (Figure 4A). This finding suggests that the proposed hybrid strategy could potentially be a more efficient method for delivering cargo molecules into cells beyond immune cells. Further investigations in future studies are warranted to explore the broader applicability of this approach in various cell types and contexts. The fact that both methods resulted in comparable cell viability implies that the HMEP protocol can achieve enhanced delivery efficiency without compromising the overall viability of the cells. This slight improvement in delivery efficiency can be attributed to the mechanical membrane disruption of the plasma membrane, which has a thickness of ~3.5 nm, leading to an augmented cargo influx. This is consistent with the previous studies demonstrating that mechanical membrane disruption can enhance the cellular uptake of cargo molecules [23, 36]. It has also been shown that mechanical disruption of the plasma membrane results in a more diffusive mode of delivery [33]. This can result in a more uniform and consistent distribution of cargo within intracellular space. The combination of these factors underscores the promise and versatility of the HMEP protocol for applications in immunotherapy and other biomedical fields, where maintaining high cell viability is a critical factor and highlights the potential applications of this strategy.

To assess the impact of the cargo size on delivery efficiency, we employed the HMEP protocol to load different sizes of the FITC dextran molecules (70, 150, and 2000 kDa) inside the Jurkat cells under the optimized conditions. As shown in Figure 4B, we observed an increase in the delivery efficiency (~20%) for 70 kDa FITC dextran, which mimics a typical mid-sized protein cargo (~ 75 kDa, 13.5 nm) [21, 37]. There is a higher probability that smaller cargo may efflux back into the surrounding media before complete membrane recovery. The lower delivery efficiency observed for 4 kDa FITC dextran can be attributed to its minute size, approximately 1 nm, which could enable it to escape into the surrounding media before the membrane fully recovers (typically within 1 minute) [38]. Further investigation is necessary to better understand the underlying

diffusive mechanisms. The findings of our study revealed that the HMEP protocol is capable of efficiently delivering cargo molecules of different sizes into Jurkat cells. The delivery efficiencies for mid-sized (70 kDa) and large-sized (150 kDa and 2000 kDa) FITC dextran molecules were relatively high, with up to 62.6%, 53.5%, and 56.2%, respectively. These results suggest that the HMEP protocol has the potential to be used for delivering different types of molecules, including proteins, CRISPR/Cas9 RNP, and plasmid DNA, into target cells. In a study conducted by Dixit et al., the successful delivery of plasmid DNA into Jurkat cells was demonstrated using a microfluidic device designed for deterministic mechanoporation [39]. Additionally, Meacham et al. showcased the successful delivery of larger target molecules, including plasmid DNA, into Jurkat cells through a combination of acoustically driven shear mechanoporation and electrophoretic insertion. Their approach achieved delivery efficiencies of up to 30% for plasmid DNA loading into Jurkat cells, highlighting the significance of the synergistic effects of mechanoporation in intracellular delivery [40]. It's worth noting that our study achieved even higher delivery results (56.2%) for larger cargo, underscoring the effectiveness of the HMEP strategy in membrane permeabilization and subsequent cargo delivery. In the HMEP strategy, the observed relationship between delivery efficiency and molecular size can be attributed to the diffusion of cargo molecules across the cell membrane through transient nanopores. Larger molecules, due to their size, diffuse less through the membrane pores of the same size compared with smaller molecules, as described by the Stokes-Einstein relationship [41].

To further expand the delivery potential of the HMEP system, we successfully loaded 4 kDa FITC dextran into THP1 cells as a representative of hard-to-transfect human monocytes. We then compared the delivery outcomes of HMEP with those achieved by benchtop electroporation (Figure 4C), as both methods rely on membrane disruption as their permeabilization mechanism. Under the same experimental conditions, we were able to achieve a delivery efficiency of up to 53.8% for the 4 kDa FITC dextran molecules using the HMEP protocol. This outcome was significantly higher than the delivery efficiency achieved through electroporation alone, validating our hypothesis that a synergistic combination of mechanical and electrical shocks can indeed lead to highly efficient cargo delivery into the second immune cell model. Next, to further demonstrate the effectiveness of this delivery method in transporting cargo molecules of various sizes, we conducted a cytoplasmic transport of 70, 150, and 2000 kDa FITC dextrans into THP1 cells using the previously optimized conditions. As shown in Figure 4D, a gradual decrease in delivery efficiency was observed with an increase in the size of the cargo molecule. This indicates that larger molecules are transported through the advection mechanism rather than passive diffusion. Previously, we demonstrated the successful delivery of 2000 kDa FITC dextran into THP1 cells using microfiltroporation. When utilizing microfiltroporation alone, we achieved a delivery efficiency of 31.1% [23]. However, by employing the HMEP delivery strategy, we were able to enhance the delivery efficiency significantly, reaching up to 44.9%. This outcome underscores the synergistic effect of combining mechanical and electric shocks to increase delivery efficiency. In contrast to Jurkat cells, THP1 cells exhibited slightly higher delivery efficiencies at a flow rate of 0.5 ml min^{-1}. This suggests that a certain level of stiffness is necessary to support plasma membrane permeabilization, and THP1 monocyte-like cells have a lower mechanical stiffness than Jurkat cells. This enables them to be efficiently permeabilized through the HMEP protocol at lower flow rates [42, 43]. However, further research is needed to explore the correlation between cell stiffness and pore formation in the plasma membrane across different immune cell types.

3.4 HMEP can efficiently deliver cargo molecules into cell-based models of hematological cancers

To further expand the applicability of this delivery protocol to hard-to-transfect cell lines, we attempted to deliver 4 kDa FITC dextran into MOLM-13 cells. MOLM-13 is an acute myeloid leukemia cell line that has been widely used in several studies to evaluate the effectiveness of the therapeutics in treating the most common cancer in children, acute myeloid leukemia, which often arises from the myelodysplastic syndrome [44-46]. As shown in Figure 5A, a positive signal was observed in up to 93% of HMEP-treated MOLM-13 cells, indicating successful cytoplasmic delivery of the 4 kDa FITC dextran. Moreover, the HMEP-treated MOLM-13 cells maintained their viability and exhibited approximately 1.7 times higher delivery efficiencies than conventional electroporation results. We also attempted to load 70, 150, and 2000 kDa FITC dextran into MOLM-13 cells to demonstrate the versatility of this delivery protocol for cargoes of different sizes. Consistent with previous experiments on THP1 cells, we observed a gradual decrease in delivery efficiency as the size of the cargo was increased (Figure 5B). The HMEP protocol allowed us to achieve average delivery efficiencies of 91.8%, 84.8%, and 58.9% for loading 70, 150, and 2000 kDa FITC dextrans into MOLM-13 cells, respectively. The HMEP protocol shows promise as an effective delivery platform for various cargoes, including therapeutic agents, such as small interfering RNA and mRNA, for leukemia treatment.

In our study, we successfully applied the HMEP protocol to load different sizes of FITC dextrans into Raji cells, which are commonly used as a cell-based model of Burkitt's lymphoma [47, 48]. The HMEP protocol achieved up to 60% delivery efficiency for 4 kDa FITC dextran while maintaining cell viability (Figure 5C). We further evaluated the performance of the HMEP delivery strategy for cytoplasmic loading of mid and large-sized cargoes (70 and 2000 kDa FITC dextran) into the Raji cells. As shown in Figure 5D, we observed a decreasing trend in delivery efficiency with increasing cargo size, which is consistent with previous studies [49]. The HMEP protocol demonstrated a critical application in the uniform and efficient delivery of 2000 kDa FITC dextran across four hard-to-transfect immune cell lines, including Raji cells.

To assess the effectiveness of the HMEP approach in delivering functional biomolecules such as plasmid DNA, we attempted to load the pEGFP-C1 plasmid DNA, which has a size of 4.7 kb, into the THP1 cells. Under optimal delivery conditions, we achieved ~50% delivery efficiency after 48 hours of treatment (Figure 6). In contrast, electroporation resulted in only 31.3% of the cells expressing GFP. This may be attributed to the mechanical forces applied to the cells, which could have led to the formation of transient pores in both the plasma membrane and the nucleus, facilitating plasmid DNA delivery. Another possible explanation is that the consistent delivery achieved through microfiltroporation may have led to higher cellular uptake of plasmid DNA. A continuing discussion surrounds the mechanism by which plasmid DNA enters the nucleus upon electroporation. One perspective suggests that the electric pulse causes permeabilization of the cell membrane, allowing electrophoresis to transport plasmid DNA directly into the nucleus [50]. In contrast, another viewpoint posits that plasmid DNA initially forms aggregates at electropermeabilized regions of the plasma membrane during the electric shock and subsequently moves towards the nucleus through a biologically active process [51, 52]. Future investigations should aim to elucidate the mechanism of plasmid DNA migration into the nucleus upon electroporation and HMEP treatment.

Our results suggest that the HMEP system can potentially be used for the delivery of other functional nanostructures, such as CRISPR/Cas9 ribonucleoprotein. This could open new avenues for the development of precise gene editing and cell engineering approaches for treating various diseases, such as hematologic cancers. However, further investigations are required to fully evaluate the potential of the HMEP protocol for delivering these cargoes into different cell types and under optimized conditions.

3.5 HMEP protocol maintains functional engineered immune cells

Finally, we investigated the effect of the HMEP protocol on the functionality of the treated immune cells. To assess the cell viability and membrane integrity, we performed several downstream analyses, including LDH, MTS, and apoptosis assays 48h post-treatment. LDH leakage is considered a marker for plasma membrane damage and cell degradation. LDH is a cytoplasmic enzyme that converts lactate to pyruvate while reducing NAD+ to NADH. When LDH is released into the extracellular environment upon membrane disruption, these reactions can occur in the presence of an added tetrazolium salt, which is reduced by NADH and converted to formazan [53, 54]. As shown in Figure 7A, while MOLM-13 cells treated with electroporation and HMEP demonstrated a slightly higher level of formazan formation compared to the untreated control cells, there was no significant difference between the two treatment methods. Additionally, we performed the MTS assay to evaluate the effect of HMEP on the proliferation of the treated cells. The results indicated no significant difference in the level of formazan between HMEP and electroporated cells (Figure 7B). These results suggest that a combination of both gentle mechanical and mild electrical shock has a minimal impact on the proliferation of actively dividing cells. Furthermore, the results of the Annexin V assay suggest that the HMEP protocol does not induce significant cell death or apoptosis, which is a crucial factor for successful cell-based therapies. FITC-conjugated annexin V binds to the phosphatidylserine on the extracellular leaflet of the phospholipid bilayer [55, 56]. During apoptosis, translocation of the phosphatidylserine to the extracellular leaflet of the phospholipid bilayer takes place, making this molecule accessible to the A5 protein. As shown in Figure 7C-E, there was no significant difference in the number of apoptotic cells between the electroporated and HMEP-treated samples. This is an important finding, as cell death or apoptosis can limit the use of these cells in various applications, including regenerative medicine and cell and gene therapy. Additionally, we performed cytokine array analysis on the non-treated control and HMEP-treated samples. Cytokines serve as pivotal regulators of the immune response, functioning as signaling molecules secreted by immune cells to communicate and coordinate various aspects of the immune system activities, such as inflammation, immune cell activation, and cell proliferation [57]. The observation of reduced cytokine levels in both electroporated and HMEP-treated THP1 cells implies that the application of electric shock may exert a suppressive or inhibitory influence on cytokine production and secretion by these cells. Notably, our analysis revealed that TNF-beta (Tumor Necrosis Factor-beta) and TGF-beta1 (Transforming Growth Factor-beta 1) exhibited reduced expression levels in HMEP-treated cells when compared to electroporation-treated cells (Figure 8). The decreased expression of these cytokines in HMEP-treated cells suggests that the synergistic effect of mechanical and electric shock could activate signaling cascades that lead to the downregulation of TNF-beta and TGF-beta1. Comparing the gene expression patterns and intracellular signaling cascades induced by HMEP and electroporation may help elucidate the specific mechanisms underlying the altered secretion of TNF-beta and TGF-beta1. Prior studies have reported alterations in gene expression patterns following electroporation, which aligns with our current

findings [12, 58]. The electrical shock imparted during the process may activate cellular stress responses, possibly leading to the downregulation of cytokine production as a protective mechanism. It is noteworthy that the observed effects do not appear to compromise the overall functionality of the cells. However, a comprehensive exploration of the underlying mechanisms responsible for the observed cytokine changes is warranted. These findings shed light on the potential of the HMEP protocol as a promising alternative to electroporation, as it offers efficient and consistent cargo delivery while maintaining cell viability and functionality.

4. Conclusion

In the landscape of immune cell engineering, electroporation has long been a prominent technique. However, its significant limitation lies in the inherent heterogeneity resulting from the treatment of a bulk population of immune cells during manufacturing procedures. Addressing this critical challenge, our study presented a novel approach that combines the advantages of both mechanoporation and electroporation to improve cargo delivery into human immune cells. This hybrid approach not only enhances consistency in treatment but has also been shown to substantially improve delivery outcomes, especially when transporting cargoes of varying sizes into immune cell lines that are typically difficult to transfect. The improved delivery outcomes achieved using this strategy for loading different sizes of cargo molecules can be attributed to the diffusive cargo influx mechanism [59, 60]. The HMEP protocol achieves homogeneity by guiding individual immune cells through a precisely engineered microfiltration system featuring micropores smaller than the cell diameter. This intricate process leads to the transient formation of pores in the cell membrane, enabling the efficient delivery of biomolecules through the complementary use of gentle electric shocks.

The HMEP protocol demonstrated several advantages over conventional microfiltroporation and electroporation, such as near-clogging-free operation, low material and cell loss, and high scalability. These features position it as an ideal choice for large-scale cell processing and immunotherapy applications. Moreover, our results affirm that the HMEP protocol ensures the safety and viability of treated cells, as validated through LDH, MTS, and apoptosis assays. As we progress, future research should focus on the development of microfluidic devices equipped with electroconductive microfiltration modules, allowing continuous mechano-electroporation to further boost delivery efficiencies.

In conclusion, the HMEP protocol presents a significant step forward in the development of efficient and effective methods for delivering cargo into cells, which is crucial for advancing the development of new cell-based therapies and treatments for various diseases.

5. Acknowledgment

M.E.W. would like to acknowledge the support of the Australian Research Council through Discovery Project Grants (DP200101860). M.E.W. holds a Fellowship from the Cancer Institute New South Wales (2021CDF1148).

6. References

1. Sung, H., et al., *Global Cancer Statistics 2020: GLOBOCAN Estimates of Incidence and Mortality Worldwide for 36 Cancers in 185 Countries.* CA: A Cancer Journal for Clinicians, 2021. **71**(3): p. 209-249.

2. Bayat Mokhtari, R., et al., *Combination therapy in combating cancer.* Oncotarget, 2017. **8**(23): p. 38022-38043.

3. Poursheikhani, A., et al., *Non-coding RNAs underlying chemoresistance in gastric cancer.* Cellular Oncology, 2020. **43**(6): p. 961-988.

4. Baudino, A.T., *Targeted Cancer Therapy: The Next Generation of Cancer Treatment.* Current Drug Discovery Technologies, 2015. **12**(1): p. 3-20.

5. Riley, R.S., et al., *Delivery technologies for cancer immunotherapy.* Nature Reviews Drug Discovery, 2019. **18**(3): p. 175-196.

6. June, C.H., et al., *CAR T cell immunotherapy for human cancer.* Science, 2018. **359**(6382): p. 1361-1365.

7. Duncan, T. and M. Valenzuela, *Alzheimer's disease, dementia, and stem cell therapy.* Stem Cell Research & Therapy, 2017. **8**(1): p. 111.

8. Scheetz, L., et al., *Engineering patient-specific cancer immunotherapies.* Nature Biomedical Engineering, 2019. **3**(10): p. 768-782.

9. Jeanbart, L. and M.A. Swartz, *Engineering opportunities in cancer immunotherapy.* Proc Natl Acad Sci U S A, 2015. **112**(47): p. 14467-72.

10. Tian, Y., D. Xie, and L. Yang, *Engineering strategies to enhance oncolytic viruses in cancer immunotherapy.* Signal Transduction and Targeted Therapy, 2022. **7**(1): p. 117.

11. Burbach, B.J., et al., *Irreversible electroporation augments checkpoint immunotherapy in prostate cancer and promotes tumor antigen-specific tissue-resident memory CD8+ T cells.* Nature Communications, 2021. **12**(1): p. 3862.

12. DiTommaso, T., et al., *Cell engineering with microfluidic squeezing preserves functionality of primary immune cells in vivo.* Proceedings of the National Academy of Sciences, 2018. **115**(46): p. E10907-E10914.

13. Gao, S., et al., *Nanotechnology for Boosting Cancer Immunotherapy and Remodeling Tumor Microenvironment: The Horizons in Cancer Treatment.* ACS Nano, 2021. **15**(8): p. 12567-12603.

14. Morshedi Rad, D., et al., *A Comprehensive Review on Intracellular Delivery.* Advanced Materials, 2021. **33**(13): p. 2005363.

15. Shi, J., et al. *A Review on Electroporation-Based Intracellular Delivery*. Molecules, 2018. **23**, DOI: 10.3390/molecules23113044.

16. Stewart, M.P., et al., *In vitro and ex vivo strategies for intracellular delivery.* Nature, 2016. **538**(7624): p. 183-192.

17. Lee, J., et al., *Nonendocytic Delivery of Functional Engineered Nanoparticles into the Cytoplasm of Live Cells Using a Novel, High-Throughput Microfluidic Device.* Nano Letters, 2012. **12**(12): p. 6322-6327.

18. Sharei, A., et al., *Cell squeezing as a robust, microfluidic intracellular delivery platform.* J Vis Exp, 2013(81): p. e50980.

19. Kizer, M.E., et al., *Hydroporator: a hydrodynamic cell membrane perforator for high-throughput vector-free nanomaterial intracellular delivery and DNA origami biostability evaluation.* Lab on a Chip, 2019. **19**(10): p. 1747-1754.

20. Williams, A.R., S. Bao, and D.L. Miller, *Filtroporation: A simple, reliable technique for transfection and macromolecular loading of cells in suspension.* Biotechnol Bioeng, 1999. **65**(3): p. 341-6.

21. Stewart, M.P., R. Langer, and K.F. Jensen, *Intracellular Delivery by Membrane Disruption: Mechanisms, Strategies, and Concepts.* Chemical Reviews, 2018. **118**(16): p. 7409-7531.

22. Yen, J., et al., *TRIAMF: A New Method for Delivery of Cas9 Ribonucleoprotein Complex to Human Hematopoietic Stem Cells.* Scientific Reports, 2018. **8**(1): p. 16304.

23. Morshedi Rad, D., et al., *Microengineered filters for efficient delivery of nanomaterials into mammalian cells.* Scientific Reports, 2022. **12**(1): p. 4383.

24. Segeritz, C.-P. and L. Vallier, *Chapter 9 - Cell Culture: Growing Cells as Model Systems In Vitro*, in *Basic Science Methods for Clinical Researchers*, M. Jalali, F.Y.L. Saldanha, and M. Jalali, Editors. 2017, Academic Press: Boston. p. 151-172.

25. De Schutter, E., et al., *Plasma membrane permeabilization following cell death: many ways to dye!* Cell Death Discovery, 2021. **7**(1): p. 183.

26. Kamiloglu, S., et al., *Guidelines for cell viability assays.* Food Frontiers, 2020. **1**(3): p. 332-349.

27. Backlund, C.M., et al., *Protein and Antibody Delivery into Difficult-to-Transfect Cells by Polymeric Peptide Mimics.* ACS Applied Bio Materials, 2020. **3**(1): p. 180-185.

28. Owen, D.M., et al., *Dynamic organization of lymphocyte plasma membrane: lessons from advanced imaging methods.* Immunology, 2010. **131**(1): p. 1-8.

29. Raes, L., et al. *Gold Nanoparticle-Mediated Photoporation Enables Delivery of Macromolecules over a Wide Range of Molecular Weights in Human CD4+ T Cells*. Crystals, 2019. **9**, DOI: 10.3390/cryst9080411.

30. O'Dea, S., et al., *Vector-free intracellular delivery by reversible permeabilization.* PLOS ONE, 2017. **12**(3): p. e0174779.

31. Zaharoff, D.A., et al., *Mechanistic analysis of electroporation-induced cellular uptake of macromolecules.* Exp Biol Med (Maywood), 2008. **233**(1): p. 94-105.

32. Kim, J.A., et al., *A novel electroporation method using a capillary and wire-type electrode.* Biosensors and Bioelectronics, 2008. **23**(9): p. 1353-1360.

33. Ding, X., et al., *High-throughput nuclear delivery and rapid expression of DNA via mechanical and electrical cell-membrane disruption.* Nature Biomedical Engineering, 2017. **1**(3): p. 0039.

34. Zhao, N., et al., *Transfecting the hard-to-transfect lymphoma/leukemia cells using a simple cationic polymer nanocomplex.* J Control Release, 2012. **159**(1): p. 104-10.

35. Ayyadevara, V.S.S.A. and K.-H. Roh, *Calcium enhances polyplex-mediated transfection efficiency of plasmid DNA in Jurkat cells.* Drug Delivery, 2020. **27**(1): p. 805-815.

36. Zhao, W., et al., *Studying the Nucleated Mammalian Cell Membrane by Single Molecule Approaches.* PLOS ONE, 2014. **9**(5): p. e91595.

37. Erickson, H.P., *Size and Shape of Protein Molecules at the Nanometer Level Determined by Sedimentation, Gel Filtration, and Electron Microscopy.* Biological Procedures Online, 2009. **11**(1): p. 32.

38. Sharei, A., et al., *Plasma membrane recovery kinetics of a microfluidic intracellular delivery platform.* Integr Biol (Camb), 2014. **6**(4): p. 470-5.

39. Dixit, H.G., et al., *Massively-Parallelized, Deterministic Mechanoporation for Intracellular Delivery.* Nano Letters, 2020. **20**(2): p. 860-867.

40. Meacham, J.M., et al., *Enhanced intracellular delivery via coordinated acoustically driven shear mechanoporation and electrophoretic insertion.* Scientific Reports, 2018. **8**(1): p. 3727.

41. Liu, A., et al., *Microfluidic generation of transient cell volume exchange for convectively driven intracellular delivery of large macromolecules.* Mater Today (Kidlington), 2018. **21**(7): p. 703-712.

42. Liu, Y., et al., *Cell Softness Prevents Cytolytic T-cell Killing of Tumor-Repopulating Cells.* Cancer Research, 2021. **81**(2): p. 476-488.

43. Tomeh, M.A., et al., *Stiffness-tuneable nanocarriers for controlled delivery of ASC-J9 into colorectal cancer cells.* Journal of Colloid and Interface Science, 2021. **594**: p. 513-521.

44. Matsuo, Y., et al., *Two acute monocytic leukemia (AML-M5a) cell lines (MOLM-13 and MOLM-14) with interclonal phenotypic heterogeneity showing MLL-AF9 fusion resulting from an occult chromosome insertion, ins(11;9)(q23;p22p23).* Leukemia, 1997. **11**(9): p. 1469-1477.

45. He, W., et al., *Discovery of siRNA Lipid Nanoparticles to Transfect Suspension Leukemia Cells and Provide In Vivo Delivery Capability.* Molecular Therapy, 2014. **22**(2): p. 359-370.

46. Buteyn, N.J., et al., *Activation of the Intracellular Pattern Recognition Receptor NOD2 Promotes Acute Myeloid Leukemia (AML) Cell Apoptosis and Provides a Survival Advantage in an Animal Model of AML.* J Immunol, 2020. **204**(7): p. 1988-1997.

47. Zhou, S., et al., *Intracellular pH-responsive and rituximab-conjugated mesoporous silica nanoparticles for targeted drug delivery to lymphoma B cells.* J Exp Clin Cancer Res, 2017. **36**(1): p. 24.

48. Li, L., et al., *Drug-free albumin-triggered sensitization of cancer cells to anticancer drugs.* J Control Release, 2019. **293**: p. 84-93.

49. Joo, B., et al., *Highly Efficient Transfection of Human Primary T Lymphocytes Using Droplet-Enabled Mechanoporation.* ACS Nano, 2021. **15**(8): p. 12888-12898.

50. Escoffre, J.-M., et al., *What is (still not) known of the mechanism by which electroporation mediates gene transfer and expression in cells and tissues.* Molecular biotechnology, 2009. **41**: p. 286-295.

51. Klenchin, V., et al., *Electrically induced DNA uptake by cells is a fast process involving DNA electrophoresis.* Biophysical journal, 1991. **60**(4): p. 804-811.

52. Weaver, J.C., et al., *A brief overview of electroporation pulse strength–duration space: A region where additional intracellular effects are expected.* Bioelectrochemistry, 2012. **87**: p. 236-243.

53. Krieg, A.F., L.J. Rosenblum, and J.B. Henry, *Lactate Dehydrogenase Isoenzymes : A Comparison of Pyruvate-to-Lactate and Lactate-to-Pyruvate Assays.* Clinical Chemistry, 1967. **13**(3): p. 196-203.

54. Uchide, N., et al., *Lactate Dehydrogenase Leakage as a Marker for Apoptotic Cell Degradation Induced by Influenza Virus Infection in Human Fetal Membrane Cells.* Intervirology, 2009. **52**(3): p. 164-173.

55. van Engeland, M., et al., *Annexin V-Affinity assay: A review on an apoptosis detection system based on phosphatidylserine exposure.* Cytometry, 1998. **31**(1): p. 1-9.

56. Logue, S.E., M. Elgendy, and S.J. Martin, *Expression, purification and use of recombinant annexin V for the detection of apoptotic cells.* Nature Protocols, 2009. **4**(9): p. 1383-1395.

57. Dinarello, C.A., *Historical insights into cytokines.* European Journal of Immunology, 2007. **37**(S1): p. S34-S45.

58. Mukherjee, P., et al., *Single cell transcriptomics reveals reduced stress response in stem cells manipulated using localized electric fields.* Materials Today Bio, 2023. **19**: p. 100601.

59. Smith, K.C., et al., *Emergence of a large pore subpopulation during electroporating pulses.* Bioelectrochemistry, 2014. **100**: p. 3-10.

60. Weaver, J.C., et al., *A brief overview of electroporation pulse strength–duration space: A region where additional intracellular effects are expected.* Bioelectrochemistry, 2012. **87**: p. 236-243.

7. List of Figures

Figure 1. HMEP delivery platform. Schematic representation of the HMEP system consisting of sequential (A) electrical disruption and mechanical delivery or (B) mechanical disruption followed by electrical delivery. This figure was generated using Biorender software (https://biorender.com/).

Figure 2. Treatment sequence optimization in HMEP platform. Jurkat cells demonstrated higher cell viability and delivery efficiency when subjected to mechanical disruption followed by electrical delivery (mechanoporation → electroporation) compared to electrical disruption followed by mechanical delivery (electroporation → mechanoporation). NC: no-treatment control; Endo: endocytosis; EP: electroporation; Mechano: mechanoporation. **** indicates the *P*-value<0.0001 (N=3).

Figure 3. Optimization of the HMEP delivery system. Since the HMEP strategy combines the effect of mechanical tension and electric shock, we started with optimizing each unit separately. The optimal electroporation (A) and mechanoporation (B) conditions were achieved at 1.35 kV, 10 ms, 3×, and 0.5-1 ml min^{-1}, respectively. As depicted in the schematic of the HMEP system (C), the optimal sequence of the treatment was found to be mechanoporation prior to the electroporation. This plan was generated using Microsoft PowerPoint. Next, we tested the HMEP system under various flow rates while keeping the electroporation conditions constant (D). The

optimal delivery of 4 kDa FITC dextran into Jurkat cells was achieved at the flow rates of 0.5 and 1 ml min^{-1}.

Figure 4. Validating the delivery performance of the HMEP method using hard-to-deliver immune cell models. A) The HMEP protocol could successfully increase the cytoplasmic loading of 4 kDa FITC dextran into the Jurkat cells compared to the benchtop electroporation. B) The HMEP protocol was also used to deliver other sizes of the FITC dextran molecules to highly viable Jurkat cells, with delivery efficiencies as high as 60%. C, D) These plans demonstrate successful delivery of small-sized cargo (4 kDa FITC dextran) (C) and mid- and large-sized cargo representatives (70, 150, and 2000 kDa FITC-dextran) (D) into the THP1 cells. FD: FITC-dextran. Endo: endocytosis, EP: electroporation. **, ***, and **** indicate *P*-values <0.01, 0.001, and 0.0001, respectively (N=3).

Figure 5. Demonstrating the versatility of the HMEP method through testing various cell-based models of hematological disorders. A) More than 80% of the MOLM-13 cells, a cell-based model of acute myeloid leukemia, were loaded with the 4 kDa FITC-dextran using the HMEP delivery platform. B) Although high delivery efficiency was achieved for loading various sizes of the FITC dextran molecules, a decreasing trend in delivery efficiency with increasing cargo size was observed. C, D). Raji cells, as a cell-based model of B cell malignancies, were permeabilized and loaded with 4 (C), 70, and 2000 kDa (D) FITC dextran molecules, further validating the delivery performance of the HMEP protocol. FD: FITC dextran. Endo: endocytosis, EP: electroporation. **, ***, and **** indicate *P*-values <0.01, 0.001, and 0.0001, respectively (N=3).

Figure 6. Plasmid DNA delivery via the HMEP approach. A, B) The pEGFP-C1 plasmid (4.7 kb) was loaded into the THP1 cells via electroporation and HMEP strategy. Endo: endocytosis, EP: electroporation, and HMEP: hybrid mechano-electroporation. * indicate *P*-values <0.05.

Figure 7. Evaluating the effect of the HMEP delivery system on cell viability and functionality. A) The LDH assay demonstrated no significant difference between the MOLM-13 cells treated with electroporation and HMEP. B) The MTS assay 48h post-delivery revealed that the proliferation of the MOLM-13 cells was minimally affected through the HMEP delivery process. C-E) These plans indicate the mean fluorescence intensity and the number of apoptotic cells in the population of no-treatment control (C), electroporated (D), and HMEP-treated (E) cells. NC: no-treatment control, EP: electroporation, HMEP: hybrid mechano-electroporation.

Figure 8. Cytokine profiling of EP and HMEP-treated cells. A, B) The images of cytokine array blots performed for EP and HMEP treated samples. The top left and bottom right dots are positive control samples. C) Heatmap depicting the mean pixel density for 23 human antibody targets.

8. List of tables

Table 1. Optimizing the electroporation conditions for loading 4 kDa FITC dextran into the THP1 cells as a representative of human monocytes.

Table 2. Optimizing the electroporation conditions for loading 4 kDa FITC dextran into the Jurkat cells as a representative of human T lymphocytes.

Table 3. Summary of the HMEP delivery protocol.

Figure 1

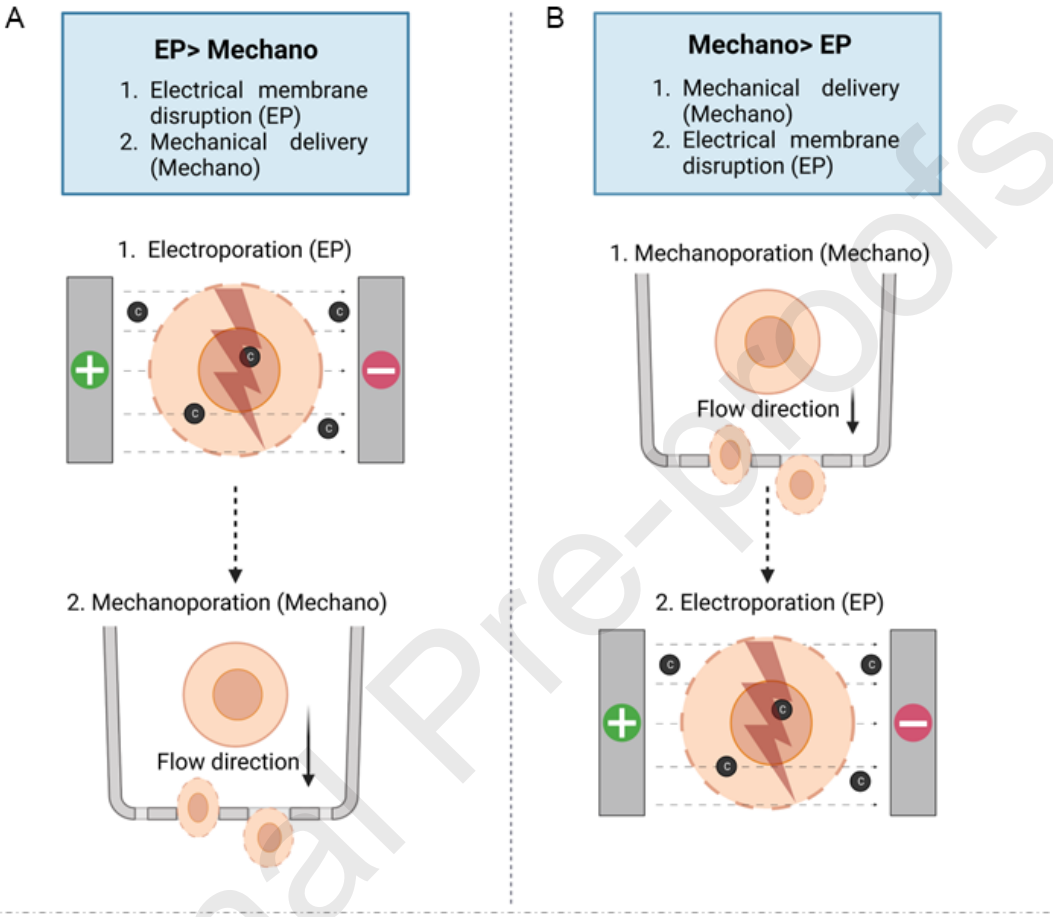

Figure 2

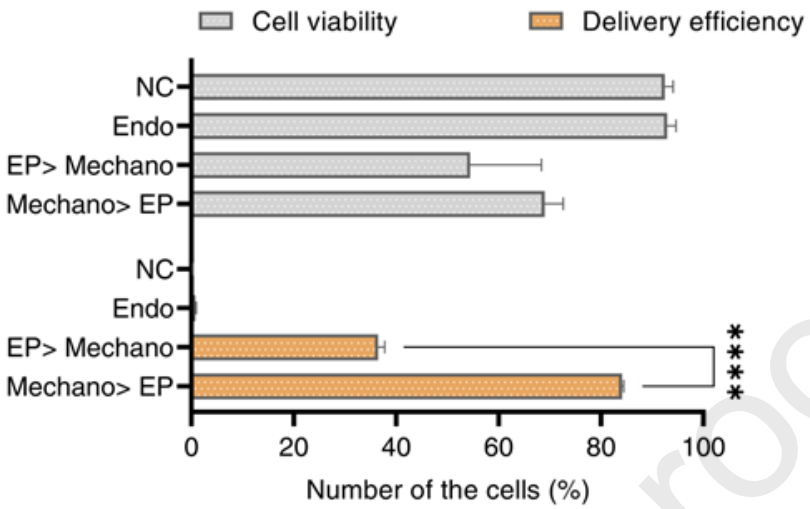

Figure 3

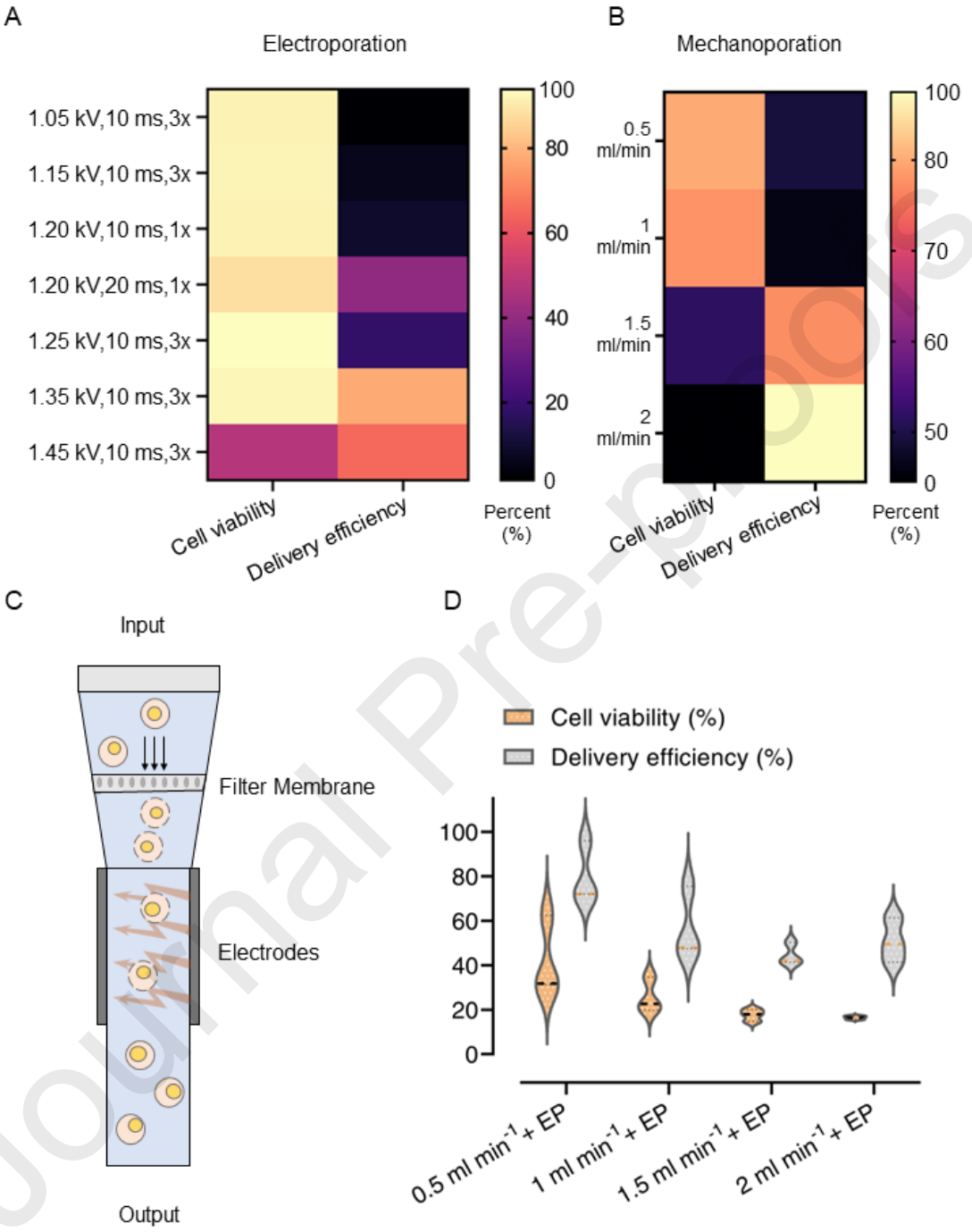

Figure 4

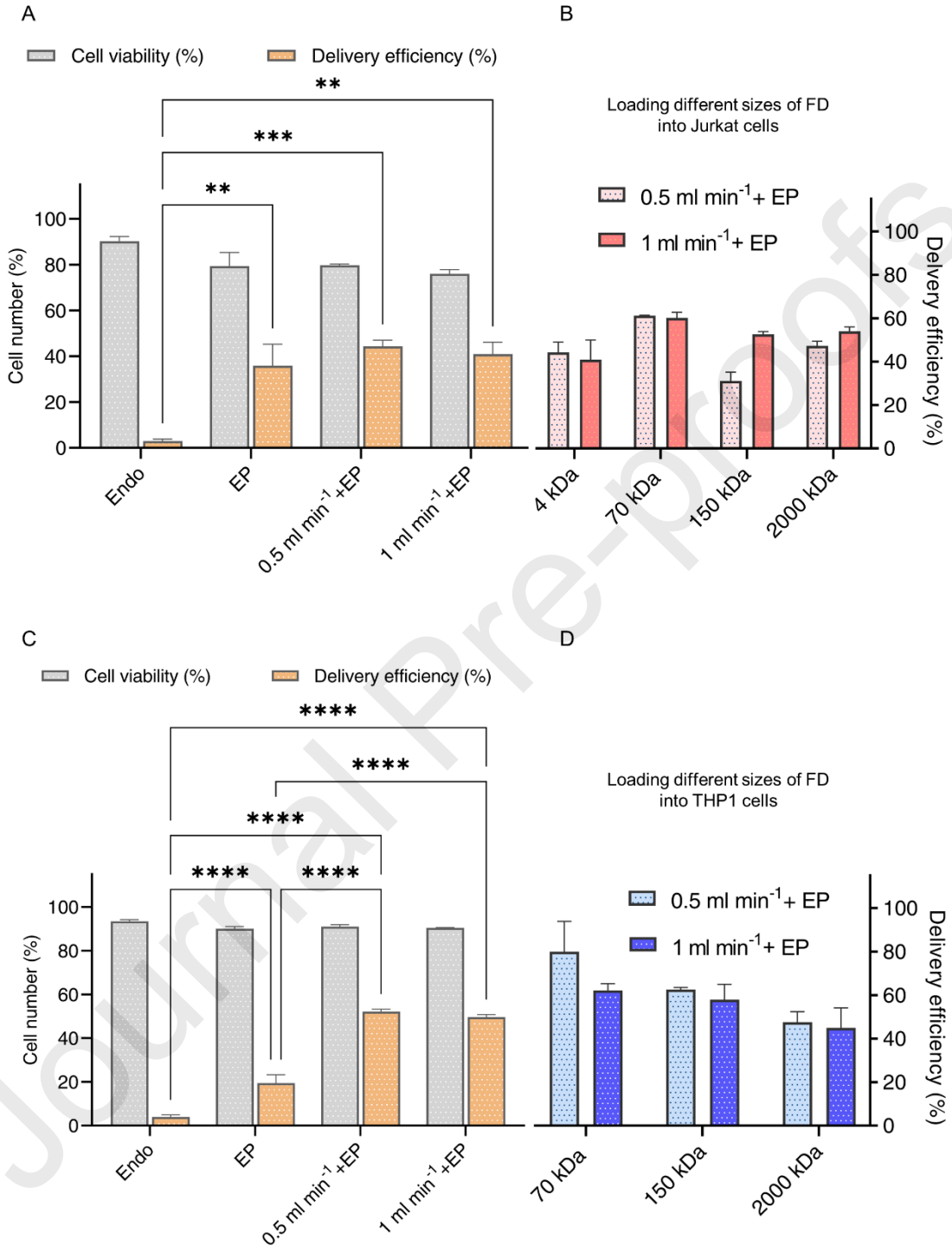

Figure 5

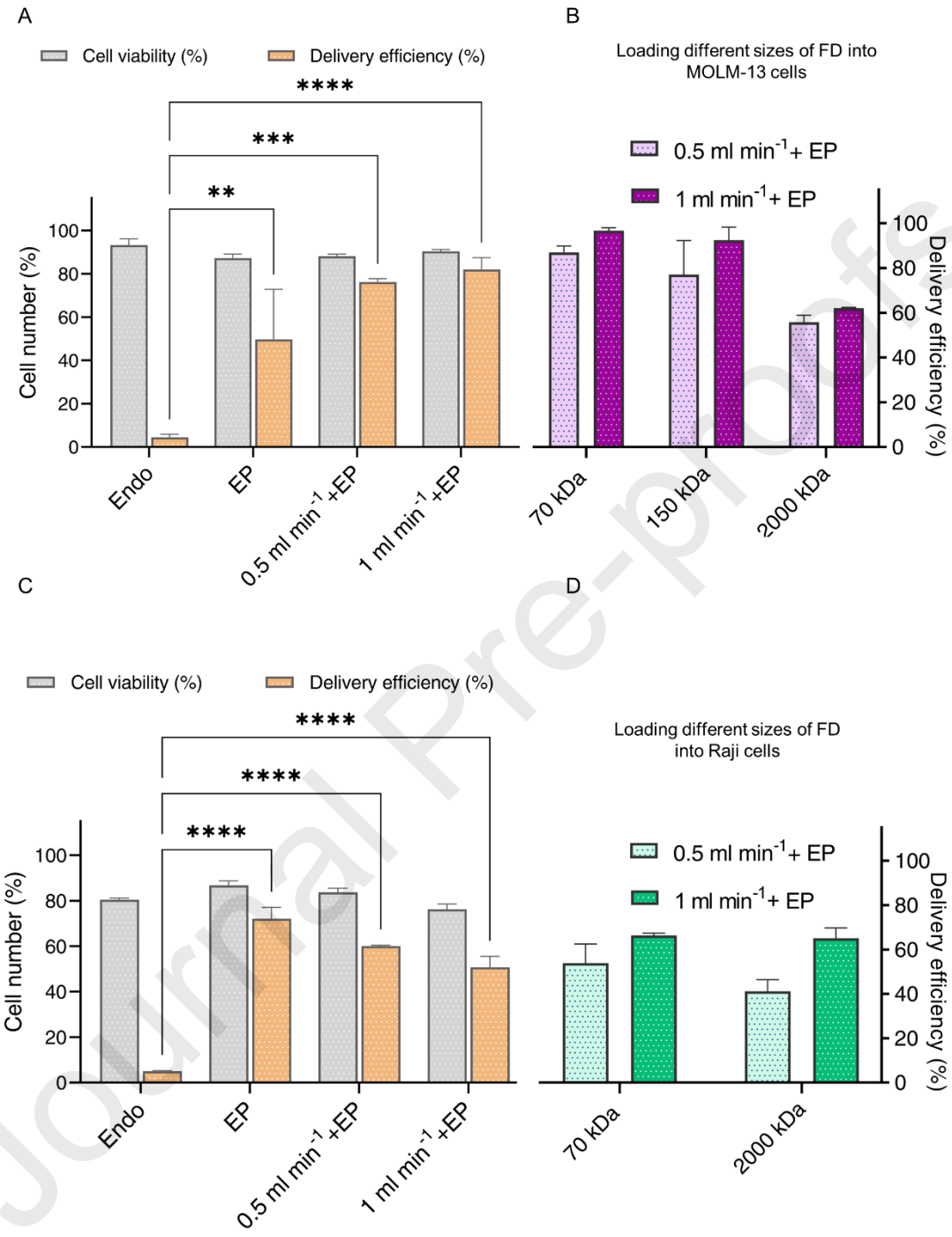

Figure 6

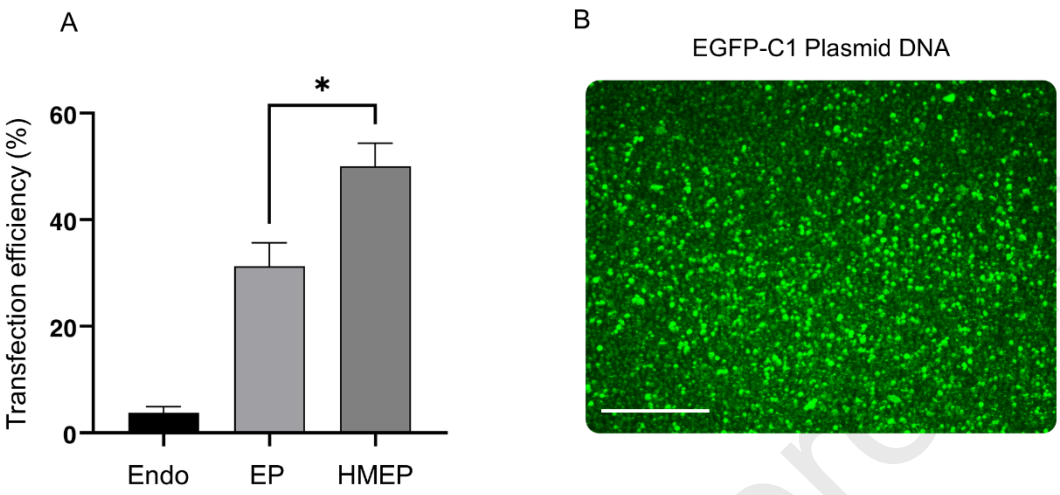

Figure 7

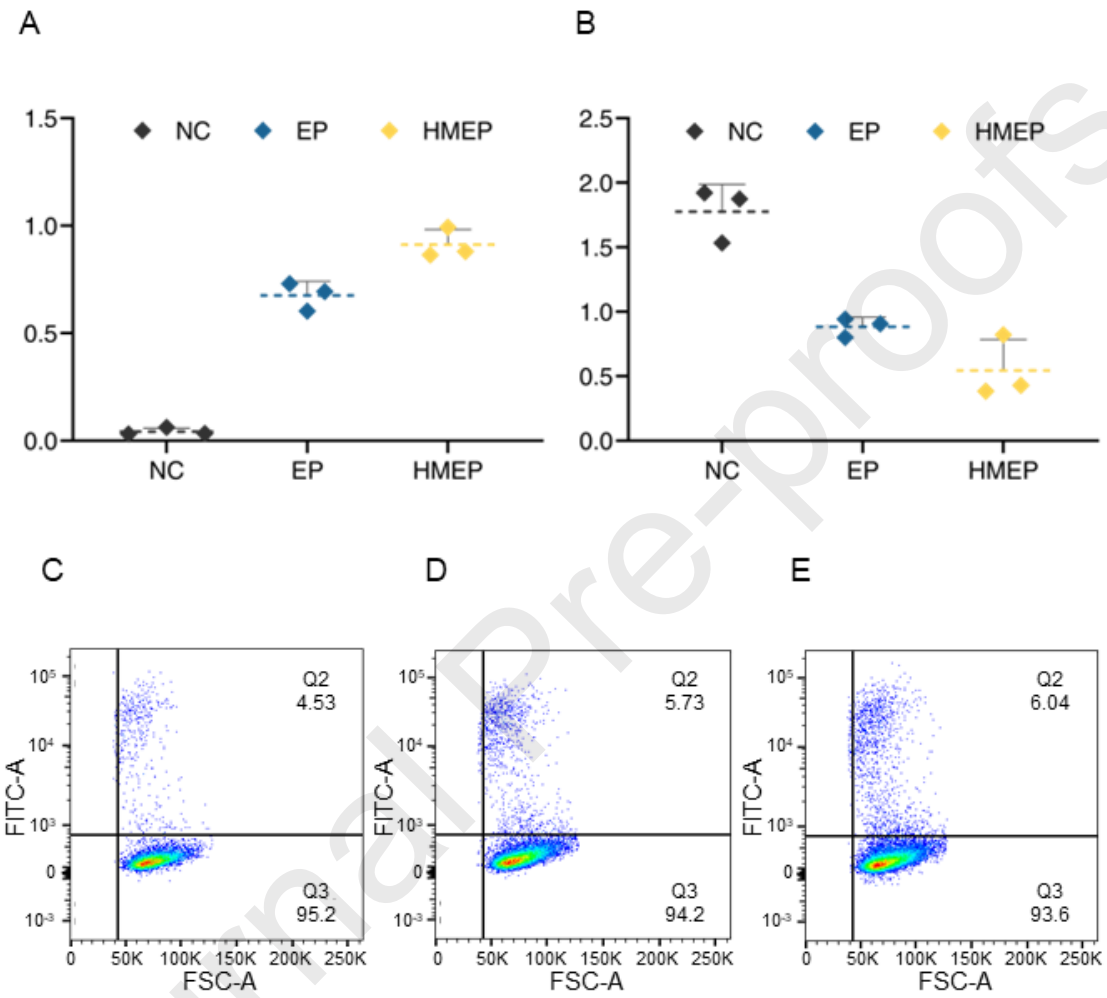

Figure 8

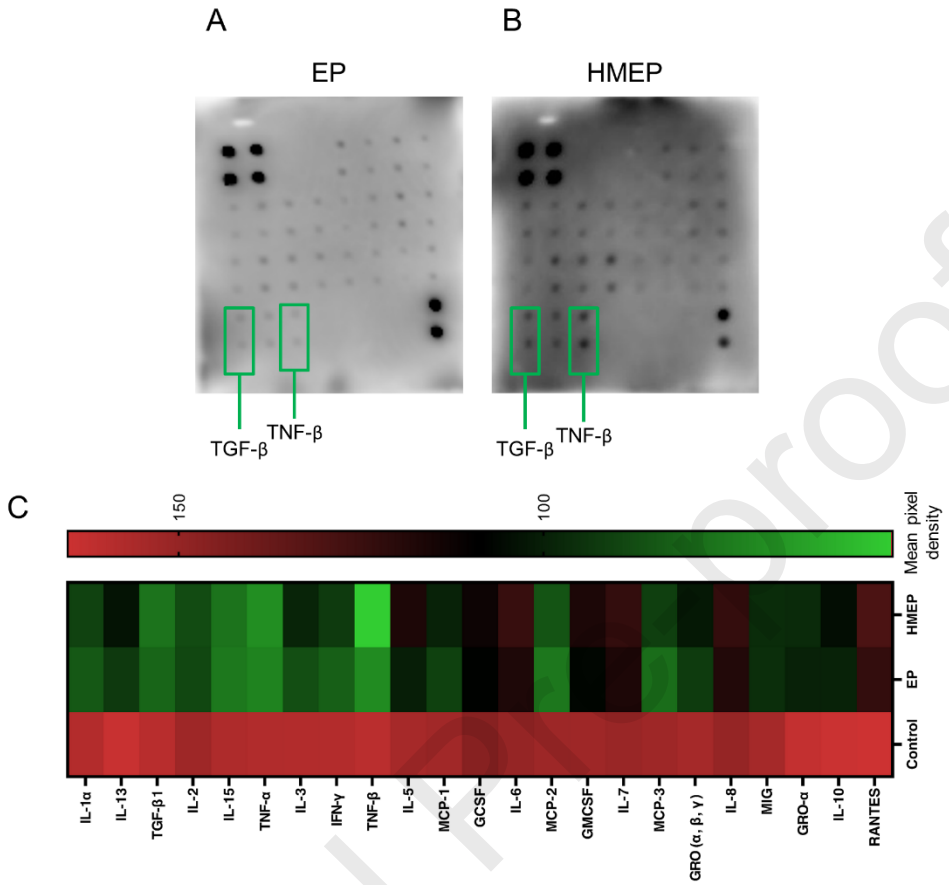

Table 1. Electroporation optimization for loading 4 kDa FITC dextran into Jurkat cells.

Sample condition	Avg. cell viability (%)	Avg. delivery efficiency (%)
Negative control	90.10	0.00
Endocytosis	91.10	2.40
1.05 kV, 10 ms, 3×	57.43	9.30
1.15 kV, 10 ms, 3×	65.47	61.10
1.25 kV, 10 ms, 3×	67.53	84.23
1.35 kV, 10 ms, 3×	70.97	95.10

1.45 kV, 10 ms, 3×	61.10	92.33

Table 2. Electroporation optimization for loading 4 kDa FITC dextran into THP1 cells.

Sample condition	Avg. cell viability (%)	Avg. delivery efficiency (%)
Negative control	94.20	0.00
Endocytosis	99.50	4.10
1.05 kV, 10 ms, 3×	84.70	48.37
1.15 kV, 10 ms, 3×	86.20	73.90
1.25 kV, 10 ms, 3×	85.20	88.63
1.35 kV, 10 ms, 3×	85.93	93.13
1.45 kV, 10 ms, 3×	65.90	79.90

Table 3. Summary of the HMEP delivery protocol.

Steps	Delivery parameter	Optimal condition
1) Mechano/microfiltroporation	Flow rate	0.5 ml min^{-1}
2) Electroporation	Electric field strength	1.35 kV, 10 ms, 3×

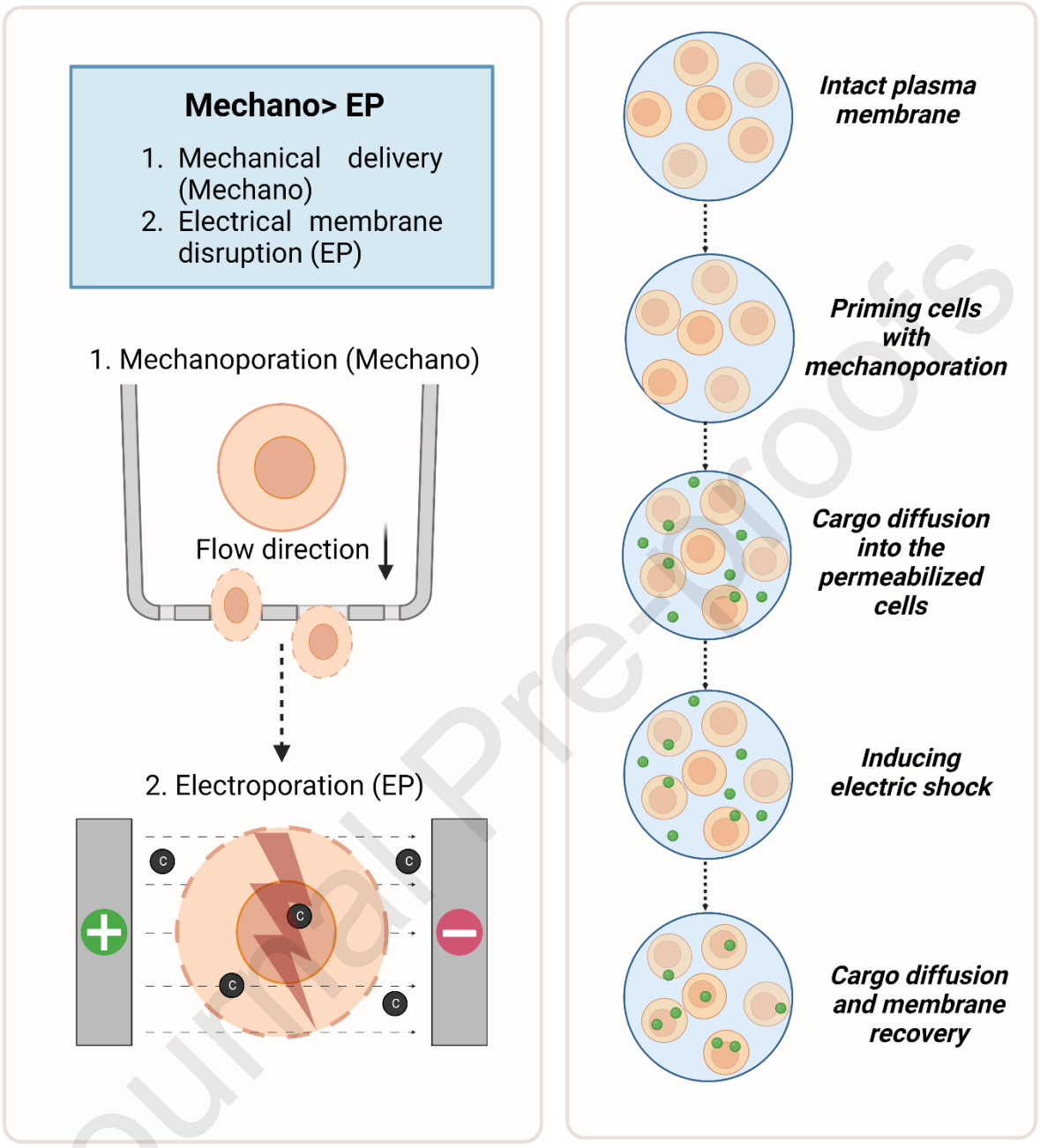

Acknowledgment and conflict of interest

M.E.W. would like to acknowledge the support of the Australian Research Council through Discovery Project Grants (DP200101860). M.E.W. holds a Fellowship from the Cancer Institute New South Wales (2021CDF1148). The authors declare no conflict of interest.

Compliance with ethics requirements

This is not applicable for this study.